Available online at www.sciencedirect.com
ScienceDirect
Carbohydrate Polymers 66 (2006) 425–434
Carbohydrate Polymers
www.elsevier.com/locate/carbpol

Influence of granule size on the flow behaviour of heated rice starch dispersions in excess water

J.C. Jacquier *, A. Kar, J.G. Lyng, D.J. Morgan, B.M. McKenna

School of Agriculture, Food Science and Veterinary Medicine, College of Life Sciences, University College Dublin, Belfield, Dublin, Ireland

Received 18 January 2006; received in revised form 14 March 2006; accepted 20 March 2006
Available online 4 May 2006

Abstract

The rheological properties of both waxy and non-waxy rice starch cooked in excess water have been studied in relation to their swelling behaviour by varying both cooking temperature (50–100 °C) and concentration (1–6%). Despite a completely different swelling behaviour with temperature, a unique linear relationship was obtained between starch weight fraction cQ, determined by means of swelling experiments and granule volume fraction Φ, assessed using particle size analysis. The rheological properties of these starch dispersions was strongly dependant on both shear rate and granule volume fraction and were reminiscent of concentrated dispersed systems with a sharp rise in relative viscosity near the maximum packing fraction. The evolution of this maximum packing fraction with shear indicated some orientation/deformation of the swollen granules. The modelling of the evolution of viscosity with shear at constant volume fraction with one relaxation mechanism allowed for the estimation of the time scale of this relaxation. The dramatic increase of this relaxation time with the cooking temperature proved that this relaxation time corresponded to deformation of the swollen granules under shear.

Keywords: Starch; Gelatinisation; Rheology; Swelling; Granule size

1. Introduction

Starch is a major component in many food systems and is widely used as a thickening agent when food manufacturers want to impart a certain mouth feel to the finished product. A wide range of cereal starches are currently used, and among them, rice starches are becoming quite popular because of their hypoallergenic properties to celiac patients, bland taste and characteristic whiteness and gloss (Zhou, Robards, Helliwell, & Blanchard, 2002).

The functional properties of starch are related to the ability of starch granules to swell and imbibe water when heated above their characteristic gelatinisation temperature in aqueous solution. This swelling is accompanied by a loss in organised structure and a leaching of soluble components, essentially amylose, into the aqueous phase, resulting in a quite complex dispersion of swollen and deformable granules in a viscous aqueous continuum (Rao, 1999). The resulting rheological properties of these dispersions are quite complex and mainly governed by the extent of starch granule swelling and concentration. Highly concentrated dispersion of poorly swollen granules often show dilatant or shear thickening behaviour, while more dilute suspensions of highly swollen granules show the characteristic pseudo-plastic or shear thinning behaviour (Bagley & Christianson, 1982). For this reason, quite a large number of investigations have been published in recent years on the relationship between the extent of starch cooking and the resulting rheological characteristics of their aqueous dispersions. Among these studies, is the pioneering work of Bagley and Christianson (1982) who established an elegant relationship between the viscosity of wheat starch dispersions and the weight fraction Q of starch granules determined macroscopically as the swelling capacity (ratio of the weight of swollen granules to the

* Corresponding author. Tel.: +353 1 716 7098; fax: +353 1 716 1149.
E-mail address: jean.jacquier@ucd.ie (J.C. Jacquier).

0144-8617/$ - see front matter © 2006 Elsevier Ltd. All rights reserved.
doi:10.1016/j.carbpol.2006.03.029

weight of dried starch). Recently, the direct method for estimating the weight fraction Q has been refined by using the dye exclusion method (Nayouf, Loisel, & Doublier, 2003), in order to take into account the interstitial water present in the sedimented granule fraction. Despite these refinements, both methods rely on the centrifugation of the starch dispersion which results can prove quite difficult to reproduce and show considerable scatter (Rao, 1999). For this reason, Rao and co-workers decided to assess the size distribution of the granules by using a laser diffraction particle size analyser and the Fraunhofer optical model. This automated microscopic method allowed for a reliable quantification of the evolution of the granule diameter with the extent of cooking in excess water for cornstarch (Okechukwu & Rao, 1995), corn and cowpea (Rao, Okechukwu, Da Silva, & Oliveira, 1997), modified maize (Da Silva, Oliveira, & Rao, 1997), tapioca (Rao & Tattiyakul, 1999), and cross-linked waxy maize starches (Meng & Rao, 2005). As all these starch dispersions were in excess water, and therefore presented negligible yield stresses, these authors analysed the flow behaviour of the suspensions using the power law model and tried to establish relationships between granule size distribution (average diameter and standard deviation) and rheological data (flow behaviour and consistency indices). In particular, they showed an inverse linear relationship between flow behaviour index and both extent of gelatinisation and the standard deviation of cornstarch granule size distribution (Okechukwu & Rao, 1995), but did not comment on the fact that the standard deviation of the size distribution was directly proportional to the average diameter of the granules, i.e. the average relative standard deviation was constant. Their conclusion on the severity of shear thickening of starch dispersions linked to the monodispersity of the dispersion is therefore open to discussion. In a later study (Da Silva et al., 1997), while comparing the granule size distributions of both cross-linked and native maize starch dispersions, these authors seem to distance themselves from their earlier observations, and attribute the progressive loss of shear thickening behaviour to the increase in granule swelling and deformability.

Also, in an analogy to the Krieger equation (Krieger & Dougherty, 1959) linking the relative viscosity of rigid sphere suspensions to their volume fraction, these authors have established empirical equations linking the consistency index K of the starch granule dispersions to the dimensionless granule diameter d ($d = D/D_o$ where D and D_o are the diameters of gelatinised and un-gelatinised starch granules, respectively). A general exponential increase of K with d was noticed in all starches studied, but with widely varying exponential factors, reflecting the maximum extent of granule swelling (Rao et al., 1997). Probably because of the empirical nature of this relationship, no further significant conclusions could be drawn between granule size, size distribution or shape, and the rheological behaviour of the dispersions.

Despite this body of work, very little is known about the rheological behaviour of rice starch dispersions in relation to the extent of granule swelling. In this study, the pasting and rheological characteristics of both waxy and non-waxy rice starches are reported, together with their swelling-solubility behaviour and the evolution of the granule size and size distribution when heated in excess water.

Because rice starch is one of the smallest of the cereal starches (Zhou et al., 2002), the microscopic evaluation of its granule size distribution using laser light diffraction cannot be performed using the Fraunhofer optical model, but instead requires the Mie's theory, in order to take into account the full diffraction spectrum. This refinement allows for a reliable determination of both granule diameter and volume, so as to enable the direct calculus of true volume fraction of starch granules.

The direct estimation of the evolution of viscosity both at high and at low shear rate with the volume fraction will enable to compare intrinsic viscosity and maximum packing fraction for both starches, thereby allowing a better understanding of the differences and similarities between these two starch varieties.

Finally, a modified equation based on Quemada's formalisms (Quemada, Flaud, & Jezequel, 1985) is presented to model the evolution of viscosity with shear at high granule volume fractions.

2. Materials and methods

2.1. Rice starches

Waxy and non-waxy (11% amylose) rice starches were obtained from Remy Industries (Leuven, Belgium). Because rice starch is known to form compound granules containing between 20 and 60 individual granules – agglomerates that can reach sizes of up to 150 μm (Zhou et al., 2002) – the starch suspensions were homogenized prior to cooking at 8000 rpm for a few minutes using a Silverson High speed mixer (Model L4RT equipped with a fine emulsion screen, Silverson Machines Limited, Chesham Bucks, UK) in order to ensure the absence of any agglomerates.

Cooking from 50 to 100 °C was performed in excess distilled water (from 1% to 6% w/w) for 30 min under mild stirring (400 rpm) to prevent excessive granule rupture. All tests were done in triplicate.

2.2. Thermodynamics of starch gelatinisation

The gelatinisation temperature and heat of gelatinisation were determined using a Differential Scanning Calorimeter (Model DSC 2010, TA Instruments Inc., Newcastle, USA). Approximately 20 mg of 30% (w/w db) raw rice starch suspension was hermetically sealed in aluminium pans (TA Instruments). A hermetically sealed empty pan was used as a reference. The scanning temperature range was 10–140 °C at a rate of 5 °C min^{-1}. The onset temperature (T_o), peak gelatinisation temperature (T_p)

and heat of gelatinisation (ΔH) were determined in triplicate.

2.3. Swelling and solubility features

The swelling power and percentage of leached solubles were determined according to Leach, McCowen, and Schoch (1958). The swelling capacity Q was calculated as the weight of the sedimented paste per gram of dry-basis starch. The notional weight fraction cQ was then calculated as the product of the swelling capacity Q by the dry starch concentration c. In effect, this product corresponds to the weight fraction of the sedimented paste in the sample.

2.4. Granule size and size distribution

Granule size distribution was determined in triplicate using a laser light scattering based particle size analyzer (Malvern Mastersizer S, Malvern Instrument Limited, Malvern, UK) fitted with a 300 RF range lens (0.05–900 μm) and a small volume sample dispersion unit. The refractive indices of water and starch were taken as 1.330 and 1.5295, respectively, with an absorption of 0.1 for starch particles (Tecante & Doublier, 1999).

The volume average diameter, $D[4,3]$ was recorded as a representative extent of granule swelling. In order to calculate the true volume fraction Φ occupied by the granules in the dispersion, the number average volume was calculated by the relation:

$$\Phi = V_g/V_T = n_g \cdot V[1,0]/V_T, \quad (1)$$

where V_g and V_T are the granule and total volumes, respectively, n_g is the number of granules and $V[1,0]$ the number average granule volume which can be obtained from $D[3,0]$ by the following equation:

$$V[1,0] = \frac{\sum_i n_i v_i}{\sum_i n_i} = \frac{\pi}{6}\frac{\sum_i n_i d_i^3}{\sum_i n_i} = \frac{\pi}{6} D[3,0]^3. \quad (2)$$

The number of granules n_g is difficult to assess at all temperatures, but in the raw state, we can write (Quemada, 1978):

$$\Phi_0 = c/d_s, \quad (3)$$

where c is the starch concentration in g/g (db) and d_s the starch density determined experimentally to be equal to (1.53 ± 0.01) g/ml (db) for both starches, in line with previously published data.

Combining Eqs. (1)–(3), we can then assess the true volume phase ratio of the starch granules at all temperatures by the expression:

$$\Phi = \Phi_0 \cdot V[1,0]/V_0[1,0] = \frac{c \cdot V[1,0]}{d_s \cdot V_0[1,0]} = \frac{c \cdot D[3,0]^3}{d_s \cdot D_0[3,0]^3}, \quad (4)$$

where the subscript 0 denotes the starch granules in the raw state.

2.5. Flow behaviour

Steady stress sweeps of cooked starch pastes in excess water (2–6% w/w) were carried out using a Rheometric Scientific SR 2000 rheometer (Rheometric Scientific Inc., Piscataway, NJ, USA) equipped with a 32 mm Couette geometry at 25 °C. The viscosity of the starch dispersions was recorded on the descending shear data in the shear range 1000–0.1 s^{-1}.

3. Results and discussion

3.1. Thermodynamics of gelatinisation

Table 1 regroups the main characteristics of thermal behaviour for the two starches studied. The peak gelatinisation temperature T_p for waxy rice starch was 67.1 °C, which is in line with previously published data (Kar, Jacquier, Morgan, Lyng, & McKenna, 2005), while the heat of gelatinisation ΔH was 15.7 J/g (db). For this starch, no melting of the starch–lipid complex was observed. In the case of non-waxy rice starch, the peak temperature (69.2 °C) and the heat of gelatinisation (13 J/g db) were quite similar to the waxy starch values. A second endotherm was observed at 100 °C, with a small enthalpy of 2 J/g db, corresponding to the melting of the starch–lipid complex (Kar et al., 2005).

3.2. Swelling behaviour

Fig. 1 shows the evolution of the water holding capacity or swelling factor Q with temperature for both starches.

In the case of waxy rice starch, the onset temperature T_o of 59 °C as determined by DSC corresponded to the start of the dramatic increase in swelling to a maximum value of around 37 g/g db at 70 °C and appears to remain relatively constant at temperatures above 75 °C. Centrifuging and siphoning off the supernatant fluid for the determination of Q are not very precise or robust procedures that contributed to the spread of data in Fig. 1, especially at high

Table 1
Thermodynamic properties of the rice starches

Starch	Gelatinisation			Starch–lipid complex		
	T_o (°C)	T_p (°C)	ΔH (J/g db)	T_o (°C)	T_p (°C)	ΔH (J/g db)
Waxy	58.9 ± 0.7	67.1 ± 0.1	15.7 ± 0.6	ND	ND	ND
Non-waxy	59.9 ± 0.8	69.2 ± 0.4	13 ± 1	93 ± 1	100.0 ± 0.1	2.0 ± 0.9

T_o and T_p are the onset and peak gelatinisation temperatures, respectively, while ΔH is the gelatinisation enthalpy. ND, not detected.

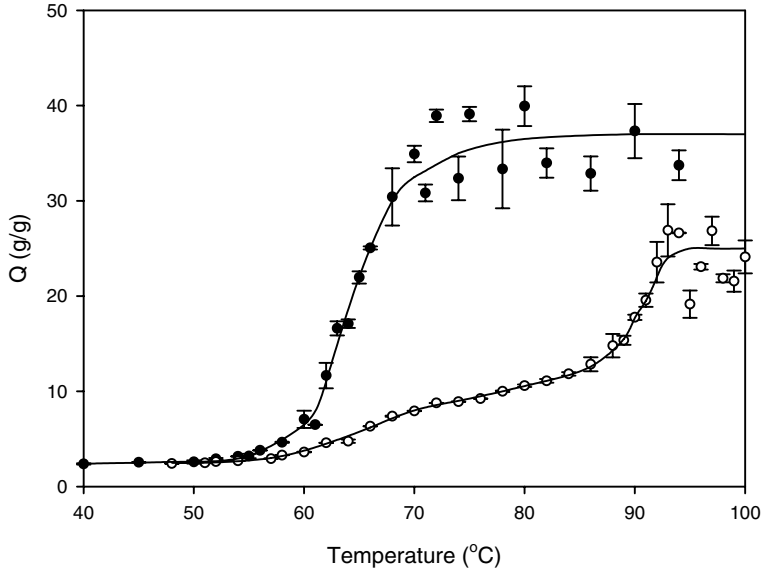

Fig. 1. Water holding capacity of rice starches as a function of cooking temperature (●, waxy; ○, non-waxy). The lines are visual fits only.

temperatures, as mentioned by other authors (Rao et al., 1997). Nevertheless, this large and monomodal increase in swelling corresponded well to the thermodynamic behaviour of the waxy rice starch. In the case of the non-waxy rice starch two-phase transitions were seen at 65 and 90 °C. As the starch was cooked from 55 °C a gradual increase in swelling power was seen (Fig. 1). At 70 °C the swelling power was ≈10 g/g db. This value remained relatively constant, forming a plateau up to 85 °C. However, as the cooking temperature was increased beyond 85 °C the water holding capacity increased dramatically forming a steep curve which appeared to plateau once again at a maximum swelling factor of 25 g/g db. Once again, as in the case of waxy rice starch, considerable spread in the values was observed at those high temperatures. But the swelling of the non-waxy starch tallies with its bimodal thermodynamic behaviour, with a slight increase in swelling at the gelatinisation temperature, followed by a second large increase in swelling when the lipid–amylose complexes melt.

3.3. Granule size distribution

Particle size analysis of starch samples involved a study of the changes in granule size (as quantified using the $D[4,3]$ sometimes referred to as the volume or mass moment mean or De Brouckere Mean Diameter (Fig. 2).

The $D[4,3]$ value of uncooked waxy rice starch is 6 μm. As cooking temperature increases, the diameter of the starch granules also increases, reaching a maximum of

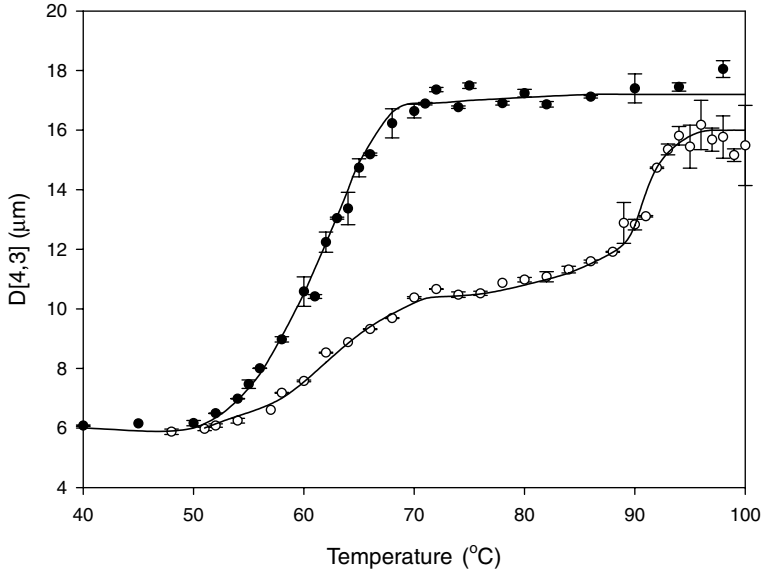

Fig. 2. Volume average diameter of rice starches as a function of cooking temperature (●, waxy; ○, non-waxy). The lines are visual fits only.

17 μm at 67 °C. Beyond this temperature no significant change is observed in granule size. In the case of the non-waxy rice starch, once again, a two-step phenomenon is seen in the granule diameter with cooking temperature. From 55 to 70 °C a relatively small increase in granule diameter from 6 to 10 μm is observed and effectively levels off until 85 °C. Upon further heating above 90 °C, the granules reach a maximum diameter of 16 μm, but there is significant spread in the data at these high temperatures, probably due to the extreme fragility of the highly swollen granules.

Despite the spread in the values for both macroscopic and microscopic determinations of the swelling of both rice starches at high temperatures, a linear relationship was found between the notional weight fraction cQ and the volume fraction Φ over the entire range of temperatures and concentrations studied, as shown in Fig. 3.

When all data for both starches (29 for waxy, 37 for non-waxy) are taken into account, a common linear relationship is derived with a good fit ($R^2 > 0.95$).

$$\Phi = (0.034 \pm 0.007) + (0.63 \pm 0.01)\mathrm{cQ}. \quad (5)$$

This fact is all the more remarkable, considering the radical differences in swelling behaviour observed for these two starches, both in terms of evolution with temperature and in the final swelling values at high temperatures. It would be interesting to see if this common relationship is observed for starches of different botanical origin.

3.4. Flow behaviour

3.4.1. Correlation of viscosity and granule volume fraction at constant shear rate

The evolution of relative viscosity under high shear (1000 s^{-1}) and low shear (0.1 s^{-1}) with the volume fraction occupied by the granules of both rice starches studied are shown on Figs. 4 and 5. Also represented on these figures are the best nonlinear fits to the Krieger–Dougherty equation (Krieger & Dougherty, 1959):

$$\eta_{\mathrm{rel}} = \frac{\eta}{\eta_{\mathrm{F}}} = \left(1 - \frac{\Phi}{\Phi_{\mathrm{m}}}\right)^{-[\eta]\Phi_{\mathrm{m}}}, \quad (6)$$

where η is the suspension apparent viscosity, η_{F} the viscosity of the suspending fluid (water in the present case), Φ the granule volume fraction, $[\eta]$ the intrinsic viscosity, and Φ_{m} the maximum granule packing fraction. Although the Krieger equation was originally derived theoretically for suspensions of rigid spherical particles for which theoretical values for $[\eta]$ and Φ_{m} are 2.5 and 0.637, respectively, it has been since successfully applied to more complex dispersions and the influence of various experimental conditions on its parameters recently reviewed (Amoros, Sanz, Gozalbo, & Beltran, 2002).

In order to check the validity of this equation in the context of starch dispersions, several precautions had to be taken to ensure some homogeneity in the quality of the dispersions. In the case of the waxy rice starch, it meant taking into account the dispersions heated to the gelatinisation temperature of 64 °C only, as to preclude major granule rupture. In the case of the non-waxy starch, granule integrity will be obtained for dispersions heated up to the melting of the amylose–lipid complex of 94 °C. Also, in order to limit granule rupture, the dispersions were heated with minimum stirring. Finally, second rheological measurements on the same dispersions were performed in order to ensure that the test had not caused irreversible damage to the dispersions.

At low shear rate, the values of Φ_{m0} and $[\eta]_0$ were determined by nonlinear regression of the evolution of the relative viscosity η_{rel0} with packing fraction Φ (experimental

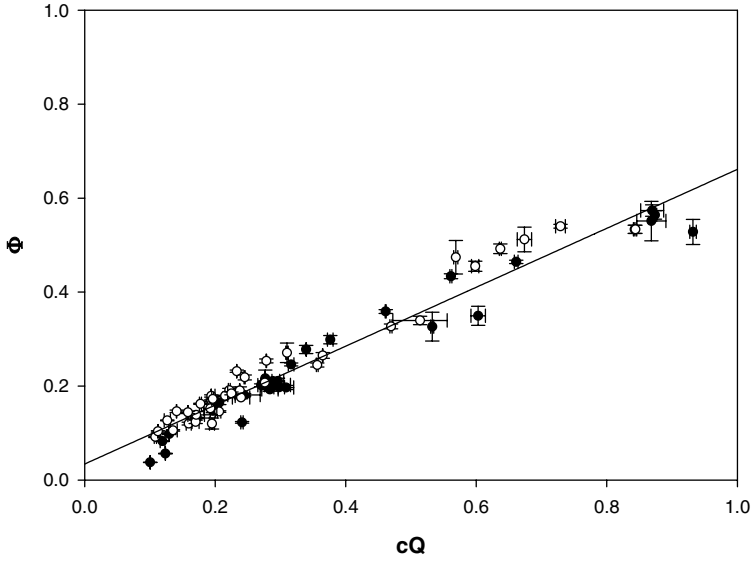

Fig. 3. Granule volume fraction Φ determined by particle size analysis as a function of mass fraction cQ assessed by swelling experiments (●, waxy; ○, non-waxy). The line is a linear regression (see text for details).

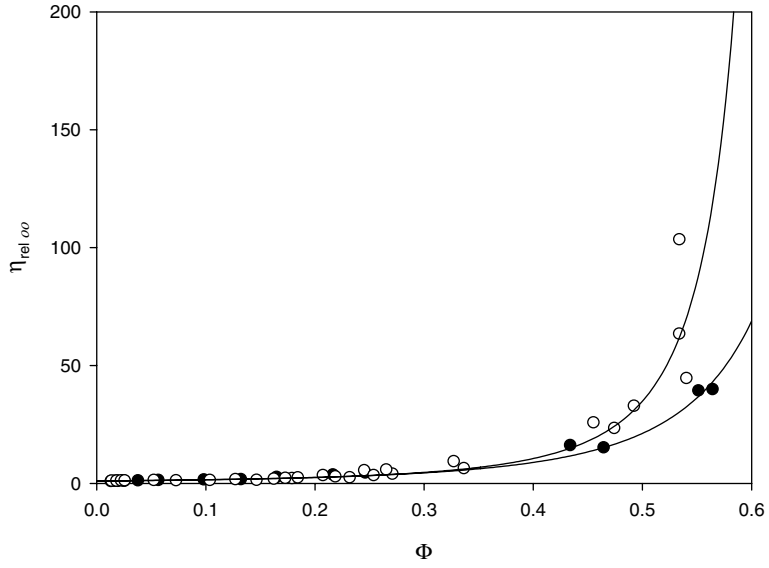

Fig. 4. Evolution of the relative viscosity at high shear with granule volume fraction (●, waxy; ○, non-waxy). The lines are nonlinear fits to the Krieger–Dougherty equation (see text for details).

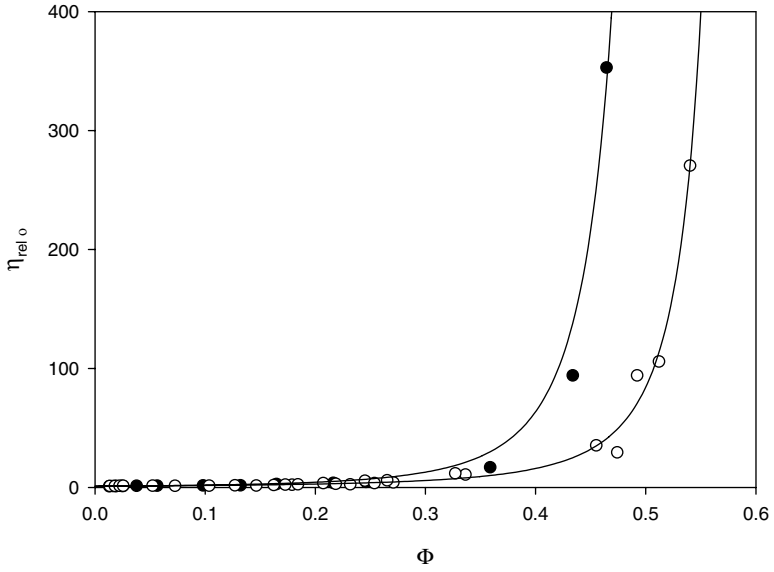

Fig. 5. Evolution of the relative viscosity at low shear with granule volume fraction (●, waxy; ○, non-waxy). The lines are nonlinear fits to the Krieger–Dougherty equation (see text for details).

points on Fig. 5) according to the Krieger–Dougherty equation (Eq. (6)).

At high shear rate, the values of $\Phi_{m\infty}$ and $[\eta]_\infty$ were equally determined by the same nonlinear regression of the evolution of the relative viscosity $\eta_{rel\infty}$ with packing fraction Φ (experimental points on Fig. 4) according to the same Krieger–Dougherty equation (Eq. (6)). These values are combined in Table 2.

Table 2
Parameters to the Krieger–Dougherty equation for both rice starches

Starch	Low shear ($\gamma = 0.1\ s^{-1}$)			High shear ($\gamma = 1000\ s^{-1}$)		
	Φ_{mo}	$[\eta]_o$	R^2	$\Phi_{m\infty}$	$[\eta]_\infty$	R^2
Waxy	0.56 ± 0.03	6.0 ± 0.5	0.98	0.84 ± 0.09	4.02 ± 0.3	0.98
Non-waxy	0.611 ± 0.07	4.3 ± 0.1	0.99	0.67 ± 0.09	3.87 ± 0.7	0.79

Φ_{mo} and $\Phi_{m\infty}$ are the maximum packing fractions at low and high shear rates, respectively, while $[\eta]_o$ and $[\eta]_\infty$ are the intrinsic viscosities at low and high shear rates, respectively.

In the high shear regime ($\gamma = 1000\ s^{-1}$), the intrinsic viscosity $[\eta]$ values for both starches appear to be similar, and smaller than at low shear ($\gamma = 0.1\ s^{-1}$). This difference is possibly indicative of a tendency of the granules to orient themselves in the direction of flow under high shear, thereby reducing their flow resistance. Similarly, comparison between high and low shear values of the maximum packing fractions for both starches indicate that $\Phi_{m\infty} > \Phi_{m0}$, as orientation of soft deformable particles under higher shear rates will lead to more compact packing. These tendencies for particle orientation in high shear flow are much more pronounced for the waxy rice starch than for the non-waxy variety, indicating perhaps a much softer and deformable granule for the waxy starch.

3.4.2. Correlation of viscosity evolution with shear

In the previous section, we saw that for a given starch suspension, both the maximum packing fraction Φ_m and the intrinsic viscosity $[\eta]$ evolve with shear, thereby reflecting particle aggregation, deformation and or orientation. It is noteworthy to mention though that the product of the maximum packing fraction by the intrinsic viscosity $\Phi_m\,[\eta]$ remains constant (Table 2) for a given starch suspension, and take the values of 3.37 and 2.6 for waxy and non-waxy rice starches, respectively. Therefore, for a given starch, the product $\Phi_m\,[\eta]$ can be said to be constant as a function of shear. Eq. (6) takes then the form :

$$\eta_{rel} = \left(1 - \frac{\Phi}{\Phi_m}\right)^{-\alpha} \tag{7}$$

with α equal to the product of the maximum packing fraction by the intrinsic viscosity $\Phi_m\,[\eta]$.

The evolution of the relative viscosity η_{rel} with shear will therefore only depend on the evolution of the maximum packing fraction Φ_m. If the state of a completely disaggregated and undeformed particles suspension is known (Quemada, 1978), one can define a structural maximum packing fraction Ψ, that depends only on particle shape and size at rest. Then we can introduce a structural parameter $\beta(\gamma)$ which displays all the effects of aggregation, orientation and deformation, and which is defined as:

$$\Phi_m = \Psi \cdot \beta(\gamma). \tag{8}$$

At rest ($\gamma \to 0$), β tends to β_0, and $\Phi_{m0} = \Psi \cdot \beta_0$, which characterise the most aggregated or non-deformed or non-oriented state, while at high shear rates ($\gamma \to \infty$), β tends to β_∞, and $\Phi_{m\infty} = \Psi \cdot \beta_\infty$, which corresponds to the most dispersed or deformed or oriented state.

A rate equation for $\beta(\gamma)$ can be written (Quemada, 1978) expressing the balance between aggregate break-down due to shear and aggregate build-up due to collisions or orientation/disorientation or deformation/un-deformation. If these processes are assumed (Quemada, 1978) to be of a relaxation type with time, they are governed by the following equations:

$$\left(\frac{d\beta}{dt}\right)_A = \tau_A^{-1} \cdot (\beta_0 - \beta), \tag{9}$$

$$\left(\frac{d\beta}{dt}\right)_D = \tau_D^{-1} \cdot (\beta - \beta_\infty), \tag{10}$$

where τ_A and τ_D are relaxation times for association and dissociation, respectively.

Under steady shear flow, a dynamical equilibrium is reached and the general balance equation takes the form:

$$\frac{d\beta}{dt} = 0 = \tau_A^{-1} \cdot (\beta_0 - \beta) - \tau_D^{-1} \cdot (\beta - \beta_\infty) \tag{11}$$

which gives the evolution of $\beta(\gamma)$ with time:

$$\beta(\gamma) = \frac{\beta_0 + \tau_A/\tau_D \cdot \beta_\infty}{1 + \tau_A/\tau_D}. \tag{12}$$

A similar set of equations can be written in the case of orientation/disorientation and deformation/un-deformation processes, but with appropriate relaxation times τ_i.

Eq. (12) therefore shows that the equilibrium value of $\beta(\gamma)$ under steady shear flow conditions only involves the ratio of the relaxation time constants that both depend on shear rate γ. Quemada (1978 and 1985) then derived a semi-empirical equation to express the evolution of this relaxation time constants ratio with shear:

$$\tau_A/\tau_D = (\tau \cdot \gamma)^p \tag{13}$$

where p is an empirical parameter which generally lies between 0 and 1 and τ a characteristic time constant for the process under study.

Inserting Eqs. (13), (12), and (8) into Eq. (7), we now have a description of the evolution of the relative viscosity with both volume fraction Φ and shear rate γ, which takes the form:

$$\eta_{rel}(\Phi, \gamma) = \left(1 - \frac{\Phi(1 + (\tau\gamma)^p)}{\Phi_{m0} + \Phi_{m\infty}(\tau\gamma)^p}\right)^{-\alpha} \tag{14}$$

It is worth mentioning here that when the system is at rest($\gamma \to 0$), Eq. (14) takes the simple form: $\eta_{rel_0} = (1 - \frac{\Phi}{\Phi_{m0}})^{-\alpha}$while at high shear rates ($\gamma \to \infty$), $\eta_{rel_\infty} = (1 - \frac{\Phi}{\Phi_{m\infty}})^{-\alpha}$.

Having estimated the maximum packing fractions at high ($\Phi_{m\infty}$) and low shear (Φ_{m0}) previously, the relative viscosity is therefore a function of the characteristic time constant of the system τ, and the granule volume fraction of the specific sample.

Figs. 6 and 7 regroup the experimental viscosity profiles for the waxy and non-waxy rice starches, respectively (symbols), as well as best non-linear fits using Eq. (14) (lines). As Figs. 6 and 7 show, the agreement between experimental and fitted flow behaviours is very good, despite the complexity of the evolution of the viscosity of these dispersions with shear.

In the case of the non-waxy rice starch (Fig. 6), starting at 60 °C, which is just above the temperature corresponding to the onset of gelatinisation as determined by DSC (Table 1), the dispersion is mainly Newtonian, with a slight

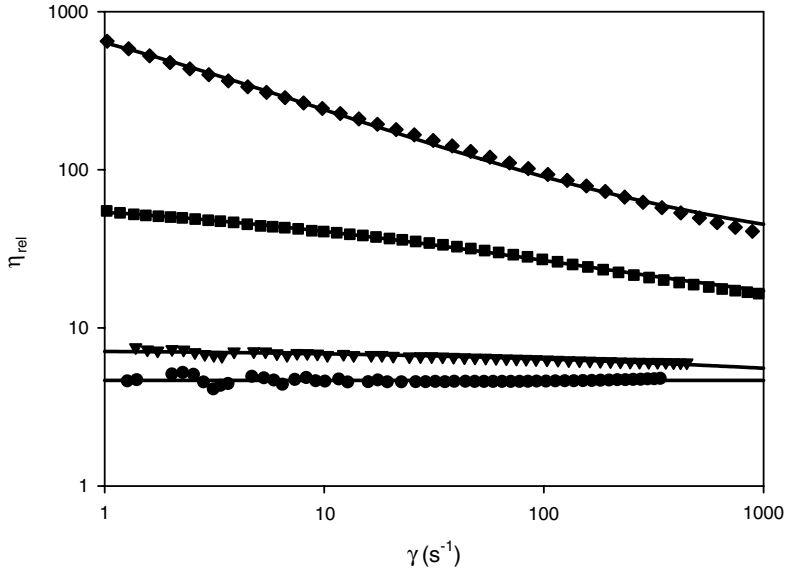

Fig. 6. Evolution of the relative viscosity of waxy rice starch with shear rate at different temperatures (●, 60 °C; ▼, 61 °C; ■, 62 °C; ♦, 63 °C). The lines are nonlinear fits to Eq. (14) (see text for details).

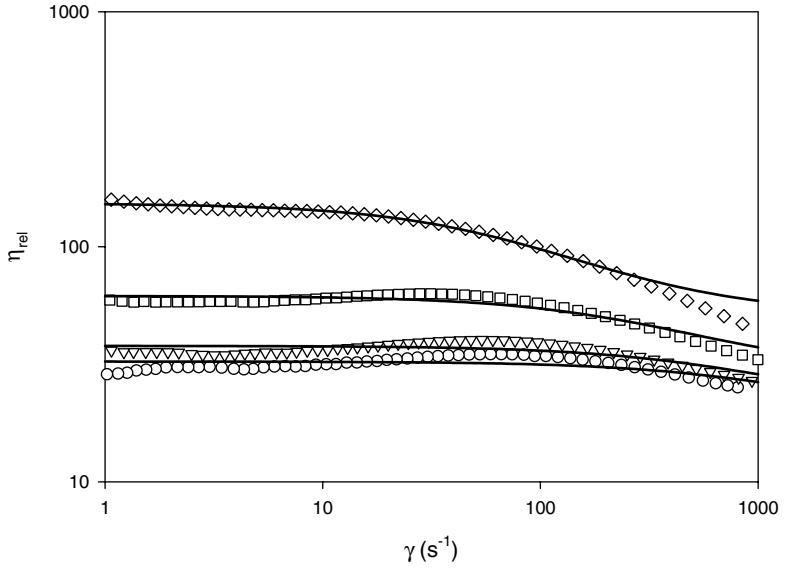

Fig. 7. Evolution of the relative viscosity of non-waxy rice starch with shear rate at different temperatures (○, 80 °C; ▽, 82 °C; □, 84 °C; ◇, 86 °C). The lines are nonlinear fits to Eq. (14) (see text for details).

up-curve at high shear rates (100–1000 s^{-1}) indicating some dilatancy. Unsurprisingly, the regression coefficient of the fit of this curve to Eq. (9) is poor as the viscosity is essentially Newtonian, i.e. constant in regard to shear rate, and the determination of the characteristic time constant of the system τ is impossible (Table 3). Nevertheless, a value of the granule volume fraction Φ can be calculated with good precision and tallies well with the experimental one.

As the cooking temperature of the waxy rice starch is raised to 63 °C, the viscosity becomes more and more shear dependant, with a marked shear-thinning behaviour. The ability of the model to predict this behaviour is excellent, as can be judged graphically (Fig. 6) and numerically (Table 3), the regression coefficients getting progressively better as the shear-thinning behaviour is more marked at higher temperatures (e.g. 62 and 63 °C).

The non-waxy rice starch was cooked between 80 and 86 °C, temperatures well above the gelatinisation temperature of this starch (Table 1) but below the melting temperature of the amylose–lipid complex (Table 1), in order to preserve granule integrity. Up to 84 °C the viscosity of these starch dispersions is quite complex, showing some shear thickening or dilatant behaviour at low shear rates and shear-thinning behaviour at high shear rates. This behaviour might be due to more than one relaxation mechanism of the system, for example, a slow aggregation

Table 3
Parameters of the fit to Eq. (14) corresponding to the evolution of the viscosity with shear

Experiment	Φ exp.	Φ calc.	τ (ms)	R^2
Waxy 60 °C	0.246 ± 0.003	0.2472 ± 0.0007	ND	0
Waxy 61 °C	0.278 ± 0.009	0.2511 ± 0.0006	0.15 ± 0.02	0.88
Waxy 62 °C	0.434 ± 0.005	0.4039 ± 0.0004	3.5 ± 0.1	0.998
Waxy 63 °C	0.55 ± 0.04	0.5089 ± 0.0007	18 ± 1	0.998
Non-waxy 80 °C	0.45 ± 0.01	0.4508 ± 0.0006	0.5 ± 0.1	0.42
Non-waxy 82 °C	0.47 ± 0.03	0.4600 ± 0.0006	0.7 ± 0.1	0.70
Non-waxy 84 °C	0.49 ± 0.01	0.4859 ± 0.0004	1.7 ± 0.2	0.91
Non-waxy 86 °C	0.540 ± 0.004	0.5227 ± 0.0004	5.7 ± 0.4	0.98

relaxation apparent at low shear rates, and a rapid deformation at short time scales apparent at high shear. But because the model of Eq. (14) is based on one relaxation mechanism only, it is obvious that the regression coefficients for the fit on these experiments will be quite low (Table 3). Nevertheless, all calculated volume fractions Φ are close to the experimental values.

For each starch, there is a systematic increase in the characteristic time constant of the system τ with the cooking temperature. If the relaxation associated with these times was due to the orientation of anisotropic granules in the direction of flow, one would imagine that the gradual increase in size of the granules due to increased temperature would keep the anisotropy somewhat constant and therefore the relaxation in the same order of timescale magnitude. On the other hand, the increase in size and fragility of the granules due to increased cooking temperature will make them more deformable. Therefore, the evolution of the calculated values of τ in Table 3 for each rice starch is well explained if this relaxation time corresponds to the deformation of the swollen granules under shear: the more fragile the starch granules become, the easier it becomes to be deformed under lower shear rates.

4. Conclusion

Despite a completely different swelling behaviour with temperature, a unique linear relationship was obtained between starch weight fraction cQ, determined by means of swelling experiments, and granule volume fraction Φ, calculated from the number average volume $V[1,0]$ of the starch granules assessed using particle size analysis. The rheological properties of these starch dispersions was strongly dependant on both shear rate and granule volume fraction and were reminiscent of concentrated dispersed systems with a sharp rise in relative viscosity near the maximum packing fraction, as predicted by the Krieger–Dougherty equation. The evolution of this maximum packing fraction with shear indicated some orientation/deformation of the swollen granules. Adapting the formalisms of Quemada, the modelling of the evolution of viscosity with shear at constant volume fraction with one relaxation mechanism allowed for the estimation of the time scale of this relaxation. The dramatic increase of this relaxation time with the cooking temperature proved that this relaxation time corresponded to deformation of the swollen granules under shear.

Acknowledgements

This research has been part-funded by Grant-in-Aid under the Food Institutional Research Measure, which is administered by the Department of Agriculture and Food, Ireland.

References

Amoros, J. L., Sanz, V., Gozalbo, A., & Beltran, V. (2002). Viscosity of concentrated clay suspensions: effect of solids volume fraction, shear stress, and deflocculant content. *British Ceramic Transactions, 101*, 185–193.

Bagley, E. B., & Christianson, D. D. (1982). Swelling capacity of starch and its relationship to suspension viscosity – Effect of cooking time, temperature and concentration. *Journal of Texture Studies, 13*, 115–126.

Da Silva, P. M. S., Oliveira, J. C., & Rao, M. A. (1997). Granule size distribution of heated modified waxy and unmodified maize starch dispersions. *Journal of Texture Studies, 28*, 123–138.

Kar, A., Jacquier, J. C., Morgan, D. J., Lyng, J. G., & McKenna, B. M. (2005). Influence of lipid extraction process on the rheological characteristics, swelling power and granule size of rice starches in excess water. *Journal of Agriculture and Food Chemistry, 53*(21), 8259–8264.

Krieger, I. M., & Dougherty, T. J. (1959). A mechanism for non-Newtonian flow in suspensions of rigid spheres. *Transactions of the Society of Rheology, 3*, 137–152.

Leach, H. W., McCowen, L. D., & Schoch, T. J. (1958). Structure of the starch granule – Swelling and solubility patterns of various starches. *Cereal Chemistry, 36*, 534–544.

Meng, Y., & Rao, M. A. (2005). Rheological and structural properties of cold-water swelling and heated cross-linked waxy maize starch dispersions prepared in apple juice and water. *Carbohydrate Polymers, 60*, 291–300.

Nayouf, N., Loisel, C., & Doublier, J. L. (2003). Effect of thermomechanical treatment on the rheological properties of crosslinked waxy corn starch. *Journal of Food Engineering, 59*, 209–219.

Okechukwu, P. E., & Rao, M. A. (1995). Influence of granule size on viscosity of cornstarch suspension. *Journal of Texture Studies, 26*, 501–516.

Quemada, D. (1978). Rheology of concentrated disperse systems. 2. A model for non-Newtonian shear viscosity in steady flows. *Rheologica Acta, 17*, 632–642.

Quemada, D., Flaud, P., & Jezequel, P. H. (1985). Rheological properties and flow of concentrated dispersed media. 1. Modelling of steady and unsteady behaviour. *Chemical Engineering Communications, 32*(1–5), 61–83.

Rao, M. A. (1999). *Rheology of fluid and semisolid foods – Principles and applications*. Gaithersburg, MD: Aspen Publishers.

Rao, M. A., Okechukwu, P. E., Da Silva, P. M. S., & Oliveira, J. C. (1997). Rheological behavior of heated starch dispersions in excess water: role of starch granule. *Carbohydrate Polymers, 33*, 273–283.

Rao, M. A., & Tattiyakul, J. (1999). Granule size and rheological behaviour of heated tapioca starch dispersions. *Carbohydrate Polymers, 38*, 123–132.

Tecante, A., & Doublier, J. L. (1999). Steady flow and viscoelastic behavior or crosslinked waxy corn starch-κ-carrageenan pastes and gels. *Carbohydrate Polymers, 40*, 221–231.

Zhou, Z., Robards, K., Helliwell, S., & Blanchard, C. (2002). Composition and functional properties of rice. *International Journal of Food Science and Technology, 37*, 849–868.